

Evidence for GR rotational frame-dragging in the light from the Sgr A* supermassive black hole

B. Aschenbach¹

Max-Planck-Institut für extraterrestrische Physik, Postfach 1312, 85741 Garching, Germany

Abstract. The analysis of flare start-times confirms the periods found years ago (Aschenbach et al., 2004) in the near-infrared and X-ray light-curves related to the Sgr A* black hole. The assignment of the frequencies found to radial and vertical epicyclic frequencies ν_r , ν_v , respectively, as well as to the Kepler orbital frequency ν_K reveals resonances of $\nu_v/\nu_r=7:2$, and $\nu_K/\nu_v=3:1$. The highest observed frequency of 10 mHz is identified as the Kepler frequency corrected by the rotational frame-dragging frequency, as expected from the Lense-Thirring effect. These frequency assignments conclude a black hole mass of $M = (4.10-4.34)\times 10^6 M_\odot$ and a spin of $a = (0.99473-0.99561)$.

Key words. black hole physics — Lense-Thirring effect — Galaxy: center — infrared: general — X-rays: general — X-rays: individual (Sgr A*)

1. Introduction

The center of our Galaxy is suspected to contain a supermassive black hole. Observationally this conjecture is based on the analysis of motions and orbit sizes of stars moving around some central mass (Schödel et al. 2002; Ghez et al. 2005; Gillessen et al. 2009). These observations suggest the presence of a fairly small volume containing a mass of several million solar masses. Mass and spin of the black hole have also been estimated from quasi-periodic oscillations (Abramowicz et al. 2004; Aschenbach et al. 2004; Aschenbach 2004) which have been suggested to be present in the near-infrared (Genzel et al.

2003) and X-ray (Aschenbach et al. 2004) light-curves of Sgr A*.

These candidate periods are suspect because of their enhanced power spectral density in at least three Sgr A* observations, which include the October 26, 2000 (*Chandra*, Baganoff et al. 2001), the October 3, 2002 (*XMM-Newton*, Porquet et al. 2004) and the near-infrared (NIR) observations of June 16, 2003 (Genzel et al. 2003). These observations were particularly interesting because they showed fairly large outbursts of Sgr A*. I have summarized the results, and I have proposed candidate period-like structures, centered around 110 s, 219 s and 1173 s (Aschenbach et al. 2004). Later measurements, both in the NIR and the X-ray band, were not conclusive on these periods. In most of the

Send offprint requests to: B. Aschenbach

cases there was no indication of a period at all, but when a time structured signal was suggested by the data, it happened to be close to the candidate period of 1100 s. This includes a 1330 s period (Bélanger et al. 2006), and a ~ 1500 s period (Meyer et al. 2008). However, each one of these observations, taken as a single event, was not and cannot be considered to be of that significance which would justify a statistically unambiguous claim of the detection of a period. But the fact that these coincidences among the light-curve observations exist as far as the putative periods are concerned, is encouraging further study.

The indication of more than one period in the light-curve data suggests the possibility that the light-curve is not dominated by just one period but that the signal is actually modulated by one or even more frequencies. So far, the analyses had to deal with light-curves which are usually subject to a large amount of noise (be it white, or red or even pink). Therefore I took the opportunity to analyse the starting times of a sequence of X-ray flares which were observed with *XMM-Newton* between 31 March and 5 April 2007, which in principle provide an independent access to periodic patterns.

2. Data and analysis

In a recent paper Porquet et al. (2008) reported for the first time a high-level X-ray flaring activity of Sgr A* observed with *XMM-Newton* between 31 March and 5 April 2007. Five flares in a row were detected. Their start-times were assessed in a quantitatively justified way by Porquet et al. (2008). They were determined to 291913503, 292051530, 292073530, 202084630, 292092330 in seconds relative to the on-board clock readings of *XMM-Newton*. The shortest separation between any two of the flares is 7700 s, and 178827 s is the widest interval. Given these times I checked each interval between any two of the flares for accommodating, as closely as possible, a natural number of

trains of a trial period covering the range from 10 s to 8000 s with a spacing of 1 ms, i.e. $\sim 8 \times 10^6$ periods were checked. The data provide 5 time-settings, or four independent time-intervals. The choice of four independent time-intervals is, however, somewhat arbitrary; one can use the time difference between two consecutive events or one can choose the time difference measured against a reference, i.e. the first flare, the second flare, etc. I decided to take all possibilities into account, which for five flares makes 10 measurements. It is obvious that these 10 time-interval measurements are not independent of each other, but this procedure tends to reduce any biases in the measurements, e.g. large measurement errors for the one or other start-time. The problem with this approach is that this procedure is likely to produce not only some solutions but also combinations of them, because of the oversampling of the information. But any eventual results can be screened for such events and eliminated afterwards.

The algorithm (see *Appendix 1*) looks for a regular flare start-time pattern, keeping in mind that most of the flares have possibly a brightness below the detection limit and are missed in the observations. The quantitative search determines the minimum residual between the observed interval and the time of either n -times or $(n+1)$ -times of the trial period. The values of the residuals are squared and added for the 10 available intervals, divided by the number of measurements (10) and after taking the square root they end up as root-mean-square (rms) value, which is then divided by the trial period. In other words, the mean relative rms-mismatch per measurement between observation and trial period is calculated. This is a dimensionless quantity, and this quantity can take values between 0 and 0.5. The inverse of that quantity I call 'goodness of fit' (GOF), which is the ratio of the trial period and the rms deviation from this trial period for the 10 time-intervals. This is NOT a significance test, it is just a search algorithm for

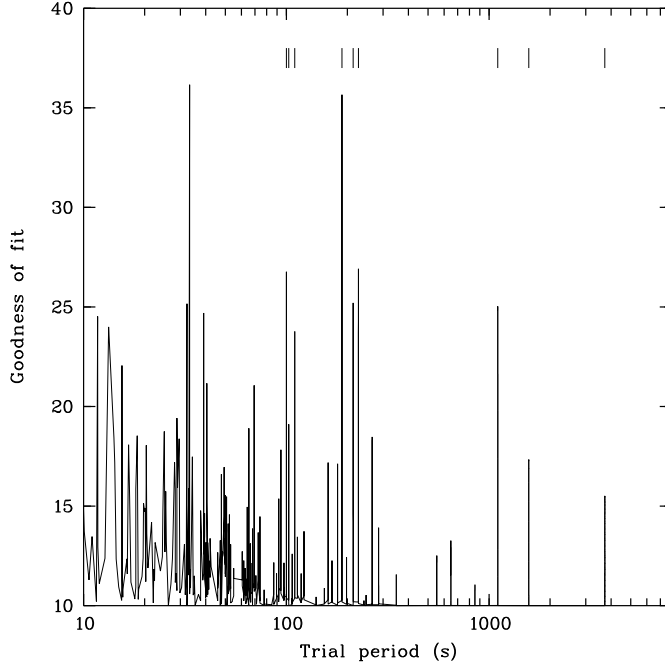


Fig. 1. Periodogram of the trial periods computed from the X-ray flare start-times of the April 2007 *XMM-Newton* observation. The tickmarks in the uppermost part of the graph delineate the positions or periods discussed in detail in the text. Data with a 'goodness of fit' value of less than 10 are not shown. For the definition of 'goodness of fit' see the text.

Table 1. Periods in the X-ray flare start-times of the April 2007 *XMM-Newton* observations.

position	period P (s)	line width $\Delta P/P$ (FWHM)	frequency ν (mHz)	mode assign.
1	100.016	1.2×10^{-4}	9.9984	$2\nu_6 + \nu_7 + \nu_9$
2	102.777	1.7×10^{-4}	9.7298	$2\nu_6 + \nu_7$
3	109.980	1.5×10^{-4}	9.0926	$2\nu_6 + \nu_9$
4	188.046	1.7×10^{-4}	5.3178	$\nu_6 + \nu_7$
5	213.650	2.6×10^{-4}	4.6806	$\nu_6 + \nu_9$
6	226.656	2.6×10^{-4}	4.4120	$\underline{\nu_6}$
7	1103.893	1.4×10^{-3}	0.90589	$\underline{\nu_7}$
8	1569.126	2.8×10^{-3}	0.63730	$\nu_7 - \nu_9$
9	3723.179	7.5×10^{-3}	0.26859	$\underline{\nu_9}$

suspects! The 'goodness of fit' versus the trial period, which I call a periodogram, is shown in Fig. 1.

The periodogram shown in Fig. 1 reveals nine prominent peaks which are listed in Table 1. The third column of Fig. 1 shows the width of the outstanding periods, which is very small, indicating that a search with a 1 ms stepping is too wide for any periods shorter than ~ 30 s. For the range with trial periods shorter than 35 s the screening was repeated with a step size of $10\mu\text{s}$. The corresponding periodogram is shown in Fig. 2.

The peak at 33.3321 re-appears, and other peaks at shorter periods show-up. These large peaks, however, have in common that the periods are exactly (to the fourth digit) given by P_1/n with n a natural number. They do not provide independent information, but none of the periods with $P > 100$ s, listed in Table 1, can be represented as a simple linear relation between any one of the listed periods.

However, when analysed in the frequency domain linear relations become apparent for $P > 100$ s, and there are just three independent frequencies left, out of which the rest can be made up by linear combinations. Because the search algorithm is in the period domain rather than in the frequency domain these three frequencies provide independent information.

The nine periods consist of two groups with one group centered around ~ 106 s and a second group centered around ~ 214 s, and two periods at ~ 1104 s (ν_7) and ~ 3723 s (ν_9), respectively, as well as their difference frequency (ν_8). Both, the group of the three frequencies around ~ 106 s and the group of the three frequencies around ~ 213 s each follow exactly the frequency relations for side band frequencies created by ν_7 and ν_9 . In principle, there are eight side band frequencies for each group and its central frequency. Apparently, only three of these nine possible frequencies show up, for each group, with a high peak in the periodogram. The central frequencies ν_c of the two frequency groups are calculated to $\nu_{c,1} = 9.3611$ mHz ($P_{c,1} = 106.825$ s) and $\nu_{c,2} = 4.68055$ mHz ($P_{c,2} = 213.65$ s). Obviously, $\nu_{c,2} = \nu_{c,1}/2$, i.e., there is just one

fundamental frequency, which is $\nu_c = \nu_{c,1}$. In summary, the observationally fundamental four flare time-intervals have provided three independent frequencies, i.e. ν_c (and $\nu_c/2$), ν_7 and ν_9 .

Of course, I have run a number of simulations assuming that five flares happen to occur at random over the entire observation time of 230 ks. GOF values as high as observed are found, for one or another period, quite frequently for periods less than about 100 s, but they tend to occur much less frequent with increasing period, so that the periods close to 1000 s and above are outstanding.

In addition, the periods showing up in the periodogram derived from the flare start-times are very much reminiscent of the periods suggested earlier to be present in the Sgr A* light-curves because of their enhanced power spectral density, i.e. the observations of October 26, 2000 (*Chandra*), October 3, 2002 (*XMM-Newton*) and the NIR flare on June 16, 2003 (for a summary see Aschenbach et al., 2004). The numbers to be compared are 106 s (110 s), 214 s (219 s) and 1104 s (1173 s). The numbers without brackets are derived from the analysis of the flare start-times taken in 2007, and the number in brackets are from the light-curves taken before 2004.

In view of this, I have not undertaken the tremendous task of calculating the probability that the observed periods are not random events, because that probability is definitely not zero. Any associated significance number just helps to decide whether to continue or stop the investigations. Because of the astonishing overlap between the periods with those, which show some enhanced power spectral density in the flares mentioned above, it is useful to investigate the possibility that the periodic structures are associated with the Sgr A* black hole.

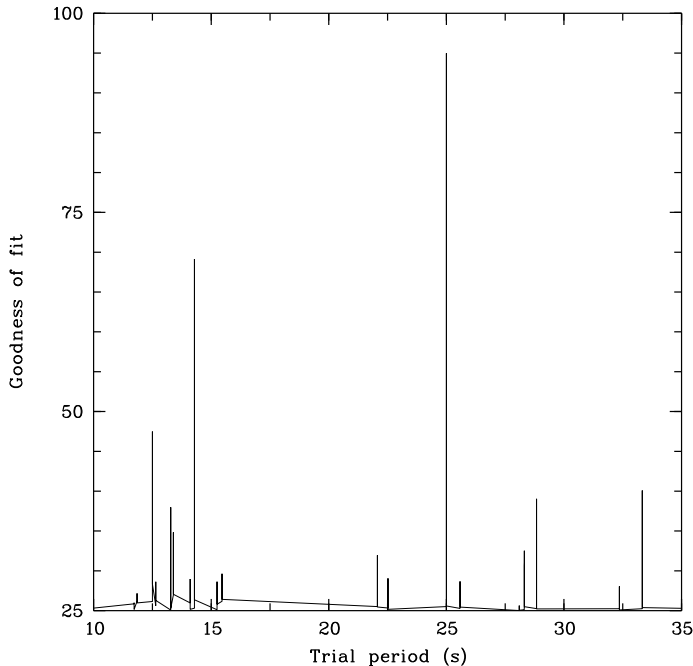


Fig. 2. Periodogram of the trial periods computed from the X-ray flare start-times of the April 2007 *XMM-Newton* observation in the range of 10 s to 35 s using a screening of 10 μ s steps. Data with a 'goodness of fit' value of less than 25 are not shown.

3. Analysis and results

The periodogram presented suggests the existence of three independent frequencies. Lacking any alternative model, which invokes more than just one frequency, I restrict the following analysis to an attempt of assigning the observed frequencies to matter oscillations somewhere in an accretion disk which is bound by a rotating black hole. I suggest to consider that a hot spot is created from a pre-existing fluctuation by resonant waves traveling through the accretion disk. These waves are in the radial direction, transporting mass and energy from the outskirts to the black hole with a frequency ν_r , and in the vertical direction, mainly raising mass density and energy density, with a frequency ν_v . The amplification of a fluctuation is most effective if the waves get into resonance, i.e. $\nu_v/\nu_r=n:m$,

with n and m natural numbers, and m as low as possible, preferentially $m=1$, or $m=2$. The resonance effect becomes even more dramatic if one or both of the waves get into resonance with the orbital motion of the initial fluctuation, which is the Kepler frequency ν_K , i.e. $\nu_K/\nu_v=k:l$, with k and l natural numbers, and l as small as possible, preferentially $l=1$ or $l=2$. Such a resonance can also be considered to hold for ν_K and ν_r . The presence of parametric resonances between the epicyclic frequencies has originally been suggested by Kluźniak and Abramowicz (2001a,b) to explain the 3:2 high frequency quasi-periodic oscillation pairs, which are observed in a number of low mass X-ray binaries most likely containing a black hole companion.

In the following I use the letters P for a period, $\nu=1/P$ for the associated frequency and Ω for the frequency expressed in GR

units, i.e. $c=G=M=1$ (c is the speed of light, G is the gravitational constant and M is the mass of the black hole). ν and Ω are related through $\Omega/\nu=2\pi GM/c^3$.

In their 1973 paper Cunningham and Bardeen studied "The optical appearance of a star orbiting an extreme Kerr black hole. Recognizing that "... the 'photon' trajectory can loop around the black hole any number of times", they concluded that there will be more than one image of the orbiting star seen by the infinitely remote observer, which are separated in time by one 'photon' orbit, and they called these images 'direct image', 'one-orbit image', 'two-orbit' image, etc. The effect on the observer is that the modulation of the light does not follow the Kepler orbital frequency but it is modified by the circular 'photon' orbit frequency Ω_{ph} such that $\Omega_1/\Omega_K=(1-\Omega_K/\Omega_{\text{ph}})^{-1}$. Ω_1 is the frequency with which the light appears to be modulated in the observer's frame. Ω_{ph} is the same frequency as the rotational frame-dragging frequency (see *Appendix 2*). As long as $\Omega_K/\Omega_{\text{ph}}\ll 1$, $\Omega_1 \approx \Omega_K$, but if this condition is violated and the frequency ratio gets closer to one, there is a large difference and Ω_1 can be boosted up to several times of Ω_K . This is the case when the black hole has a spin of $a \approx 1$, and if the Kepler orbit radius is just a few gravitational radii or less. If this happens, the modulation of the light-curve is no longer with Ω_K , and there is no frequency at the value of Ω_K . The by far highest frequency is then Ω_1 .

The frequency data shown in Table 1 suggest that $\nu_r=\nu_9$, $\nu_v=\nu_7$ and $\nu_l=\nu_c$. Using the relativistic expressions for Ω_{ph} , Ω_K , Ω_v and Ω_r (see *Appendix 2*) a best-fit reveals $P_K=1/\nu_K=368$ s if $\nu_K/\nu_v=3:1$, and $\nu_v/\nu_r=7:2$. The value of P_c was fixed at its measured value. The value of P_v was fitted to 1085.3 s instead of the measured value of 1103.9 s, which is a difference of -1.7%, and P_r was fitted to 3798.5 s instead of the measured value of 3723.2 s, which is a difference of +2.0%. The best-fit also provides the black hole mass and the black hole spin, which are $M = 4.22 \times 10^6 M_\odot$

and $a=0.99519$. The orbit resonance radius is at $r=1.49$, which is 1.115 times the radius of the innermost stable circular orbit or $R = 0.93 \times 10^{12}$ cm in physical units. An uncertainty of $\pm 2\%$ in the measured values of ν_v and ν_r each, leads to an acceptable range for the black hole mass of $4.10 \times 10^6 M_\odot \leq M \leq 4.34 \times 10^6 M_\odot$ and a range for the spin of $0.99472 \leq a \leq 0.99561$.

4. Light-curves

According to the frequencies found temporal variations of the light-curves, both in the near-infrared as well in the X-ray band, should occur. Hot-spots are periodically generated at a rate of the vertical epicyclic frequency ν_v (every 1100 s). The occurrence rate is, however, modulated by the radial epicyclic frequency $\nu_r=2\nu_v/7$, such that the flare rate varies with $\nu_v \times (1 \pm \nu_r/\nu_v)$. Accordingly, in snap-shot like observations periods can be found which vary between 850 s and 1540 s among different observations.

Because of the resonance of ν_K and ν_v , a hot-spot, once created, has the chance to be re-heated periodically, and flare again. The time separation between such flares should be exactly equal to P_v (1100 s), or $2 \times P_v$ (2200 s).

When the flares originate from two different locations of hot-spots around the orbit, the time separation between two consecutive flares can differ from P_v by as much as one orbital period, because of the optical transfer function of the black hole, which causes a delay between the hot-spot creation epoch and the time when the image passes the line of sight of the observer. The difference between the start-times of two consecutive flares is therefore somewhere between $730 \text{ s} < \Delta t_{\text{flare}} < 1470 \text{ s}$.

At last, the light-curves will be modulated by the orbital motion of the hot-spot, but at a frequency of ν_l (106 s) and $\nu_v/2$ (214 s).

5. Conclusion

The periods indicated in earlier observations of the near-infrared and X-ray light-curves from the accretion disk around the Sgr A* black hole are confirmed by the analysis of the flare start-times. The frequencies found imply resonances of 3:1 and 7:2 suggesting that radial and vertical wave oscillations as well as the Kepler frequency are involved. Taking into account the rotational frame-dragging, which should anyhow be included in such an analysis (the Lense-Thirring effect, the Cunningham-Bardeen approach), the data are consistent with the presence of a supermassive, $M = (4.10\text{--}4.34)\times 10^6 M_\odot$, and very rapidly spinning, $a = (0.99473\text{--}0.99561)$, black hole. The inclusion of rotational frame-dragging, which is one of the key features of General Relativity, is mandatory in this analysis and, of course, interpretation.

An open issue is the ad-hoc assumption that hot-spots are created from pre-existing fluctuations. The analysis presented shows that the spin of the Sgr A* black hole is very close to $a_c=0.09953$, above which the anomalous orbit velocity effect or 'Aschenbach' effect (Stuchlík et al. 2005) occurs (Aschenbach 2004). At $a_c=0.09953$, the radius derivative of the orbital velocity $\partial v^{(\Phi)}/\partial r = 0$. This condition might cause an instability in the disk, like a shear-instability, which is being amplified by the radial and vertical waves.

References

- Abramowicz, M., Kluźniak, W., McClintock, J. E. & Remillard, R. A. 2004, ApJ, 609, L63
 Aliev, A. N. & Galtsov, D. V. 1981, Gen. Rel. Grav., 13, 899
 Aschenbach, B., Grosso, N., Porquet, D. & Predehl, P. 2004, A&A, 417, 71
 Aschenbach, B. A&A, 425, 1075
 Baganoff, F. K., et al. 2001, Nature, 413, 45
 Bélanger, G., Terrier, R., de Jager, O. C., Goldwurm, A. & Melia, F. JPhCS, 54,

420

- Cunningham, J. M. & Bardeen, C. T. 1973, ApJ, 183, 273
 Genzel, R., et al. 2003, Nature, 425, 934
 Ghez, A. M., et al. 2005, ApJ, 620, 744
 Gillessen, S., et al. 2009, ApJ, 692, 1075
 Kluźniak, W. & Abramowicz, M. 2001a, Phys. Rev. Lett., submitted [astro-ph/0105057]
 Kluźniak, W. & Abramowicz, M. 2001a, Acta Phys. Pol. B, B32, 3605
 Meyer, L., et al. 2008, ApJ, 688, L17
 Porquet, D., et al. 2003, A&A, 407, L17
 Porquet, D., et al. 2008, A&A, 488, 549
 Schödel, R., et al. 2002, Nature, 419, 694
 Stuchlík, Z. 2005, Phys. Rev. D, 71 Issue 2, id. 024037

Appendix 1

A series of start-times of flares has been measured, and the time differences Δ_i between any two flares is searched for periodicities by scanning the values of Δ_i with a trial period P and a best-fitting natural number, which is either n_i or n_i+1 . The choice between n_i and n_i+1 is made by the lower residual. There are N such intervals.

$$a_i = (\Delta_i - n_i \times P)^2 \quad (1)$$

$$b_i = (\Delta_i - (n_i + 1) \times P)^2 \quad (2)$$

$$c_i = \min(a_i, b_i) \quad (3)$$

$$X = \sqrt{\frac{1}{N} \sum_{i=1}^N c_i} \quad (4)$$

The inverse of the root mean square value X divided by the trial period P is called 'goodness of fit' (GOF).

$$\text{GOF} = \frac{P}{X} \quad (5)$$

Appendix 2

There are three cyclic modes associated with black hole accretion disks, which are

the Kepler frequency (Ω_K), the disk perturbation frequencies in vertical and radial direction called vertical (Ω_V). Each frequency depends on the central mass M , the angular momentum a and the radial distance r from the center. Equations 6 to 8 show the relations (Aliev & Galtsov, 1981). Equation 9 shows the dependence on the variables for the rotational frame-dragging frequency or Ω_{ph} . The notation of $c=G=1=M$ is used. Physical length scales are in units of GM/c^2 and angular frequencies Ω are in units of c^3/GM . $r = 1$ is defined as the gravitational radius r_g .

$$\Omega_K = (r^{3/2} + a)^{-1} \quad (6)$$

$$\Omega_V^2 = \Omega_K^2 \left(1 - \frac{4a}{r^{3/2}} + \frac{3a^2}{r^2}\right) \quad (7)$$

$$\Omega_R^2 = \Omega_K^2 \left(1 - \frac{6}{r} + \frac{8a}{r^{3/2}} - \frac{3a^2}{r^2}\right) \quad (8)$$

$$\Omega_{\text{ph}} = \frac{a}{2(1+\sqrt{1-a^2})}. \quad (9)$$